

# Flow Driven Analysis of a Darrieus Water Turbine

Matjaž Fleisinger\* – Matej Vesenjāk – Matjaž Hriberšek

University of Maribor, Faculty of Mechanical Engineering, Slovenia

*The paper discusses the development of transient sliding grid based flow driven simulation procedure for a Darrieus turbine analysis. A new computational procedure is developed within the Ansys-CFX software that allows fast solutions with good accuracy of the results. With this approach it is possible to determine the turbine power curve over its whole operating range at a given flow velocity in a single simulation. This enables comparison of several different geometry parameters to find the one that extracts the most of energy of water current. The proposed procedure allows a start-up analysis of a turbine and is also suitable to run in combination with fluid-structure interaction (FSI) analysis to analyze the mechanical behavior of the turbine blades.*

**Keywords:** hydrokinetic turbine, computational fluid dynamics (CFD) simulation, flow-driven approach

## 0 INTRODUCTION

Energy of waterways is mostly extracted by means of conventional power plants. They require some kind of a dam that creates an artificial water head, which should be large enough to propel a water turbine. A few years ago, the tidal energy systems were adapted for river energy extraction, which have their origins in wind energy extraction technologies [1]. Such systems can be placed in a free stream in the same way that a wind turbine is in wind, without the need for a dam or a channel. Therefore, they extract kinetic energy of a current, where the major differences to the wind energy extraction are about 800 times greater density of water than air and slower current velocities, that are however more stable and predictable than wind. In order to improve the technology for energy extraction, the numerical simulations provide a valuable tool for numerous virtual experiments prior to the real prototypes being manufactured. The computational fluid dynamics (CFD) simulations used in this work use flow-driven approach that can consider more realistic conditions in simulation. In such simulation, the turbine rotation is governed by stream velocity from standstill onwards, which better corresponds to the real operating conditions. Because of a complex flow field around turbine blades, the use of CFD simulations is essential for better insight into flow conditions around the hydrofoils in order to improve the turbine operation, as well as for accurate performance prediction of turbine rotors.

## 1 MATERIALS AND METHODS

### 1.1 Hydrokinetic Turbines and Darrieus Turbine

Hydrokinetic turbines are designed to be installed in a stream or current, extracting kinetic energy from

the flow of water to power an electric generator without impounding or diverting the flow of the water. Conceptually, this is similar to the way wind energy conversion devices work. Considering that hydrokinetic turbines can be deployed in any water resource having sufficient velocity to drive them (between 1 and 2 m/s or even less [2]), their energy generation potential is enormous. Water resources that could be harnessed include natural streams, tidal currents, ocean currents and constructed waterways such as channels. Installation of such systems is much simpler, because they do not need dams and they can be easily moved to another location or entirely removed from the waterway. During their operation or at rest, they also do not prevent the migration of water organisms.

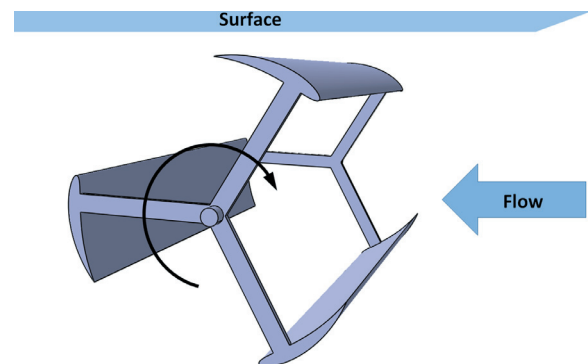


**Fig. 1.** Darrieus water turbine with horizontal axis placed in a shallow riverbed

The Darrieus turbine (Fig. 1) was invented by Georges Jean Marie Darrieus and was patented in USA in 1931 [3] and [4]. Its original intent was extraction of wind energy, so because its rotational axis was positioned vertically, in literature it is often regarded as vertical axis wind turbine (VAWT). In recent years it has been adapted for water energy extraction, where

\*Corr. Author's Address: University of Maribor, Faculty of Mechanical Engineering, Smetanova ulica 17, 2000 Maribor, Slovenia, matjaz.fleisinger@amis.net

its axis could be positioned vertically or horizontally and in both cases orthogonal to the incoming water stream. Both positions have their own benefits: in vertical position the electric generator can be mounted above water level; in horizontal position on Fig. 1 it is possible to have only one generator for the whole width of the channel. Because of the rectangular cross section of its rotor, the water Darrieus turbines can fill a larger cross-sectional area in shallow water than horizontal axis turbines with a circular cross-section. Its advantage in tidal current extraction is also the ability to extract current flowing in any direction without the need for a turn. The Darrieus turbine is also beneficial regarding blocking of the river/channel cross section, because its structure is relatively open compared to propeller turbines. The latter mainly uses an adapted Kaplan turbine rotor that requires guiding vanes or ducts for increased efficiency. The weaknesses of the Darrieus turbines on the other hand are relatively poor starting torque and its high oscillations during [3]. To avoid these disadvantages different airfoil profiles, helical blades configuration, increased number of blades or blades with variable pitch might be used.

The Darrieus turbine compared to propeller turbines has very complex flow around its blades because of its crossflow configuration, where the blades cross the global current twice every turn. The flow is undisturbed on upstream side, but on the downstream side it is already highly effected due to previous blade crossing. The angle of attack of each blade changes constantly during operation but the databases of available airfoil data (lift and drag coefficients) are limited between  $+15$  and  $-15^\circ$  [5] due to unstable operation outside this limits. Therefore the performance of a turbine cannot be estimated using simple lift and drag force equations. There are also some analytical approaches for VAWT performance prediction using different aerodynamic models (potential flow theory, vortex theory [3], [6] and [7]), but they also require airfoil coefficient data and their results are only estimations. Therefore, the computational fluid dynamics was employed allowing the study of the flow field around the turbine and to overcome the lack of previously mentioned methods. Furthermore, the CFD allows analyzing transient simulations with ability to run them as a flow driven problem. This means that the turbine starts to move and rotates due to current flow acting on its blades. The simulations of flow driven Darrieus turbine have not been shown in such detail yet.

The parametric numerical simulations also allow analyzing many different turbine design parameters,

providing an optimal configuration for a given set of design parameters. The turbine design parameters were chosen following work by Shiono et al. [8], where the turbine was experimentally tested with several different solidity parameters and current velocities. Based on previous research [9] and work by Shiono et al. the helical blade configuration was not chosen for further investigation, due to its reduced power coefficient and the difficult manufacturing procedure of such blades. The disadvantage of common computational approach for turbomachinery simulations is the need to prescribe a set of operating parameters first, such as rotational and flow velocity [10] to [13]. The main scope of this work is to validate the computational approach with a self-developed Fortran [14] routine with experimental data in a way similar to how Howell et al. [15] performed their comparison of experimental and computational results. Our simulation approach employs flow driven turbine simulation which better corresponds to real turbine operating conditions.

## 1.2 CFD and Flow Driven Motion

In order to study the performance of the Darrieus turbine computationally, the numerical model has to account for the flow phenomena in the fluid and the hydrodynamic load on the turbine blades. To obtain the flow dependent rotation of the turbine, a physically correct coupling algorithm between the fluid motion and the solid body motion has to be applied.

From the physical viewpoint, the equations describing fluid flows and heat and mass transfer are simply versions of the conservation laws of physics, namely: conservation of mass in Eq. (1) and conservation of momentum in Eq. (2) [9]:

$$\bar{\nabla} \cdot \bar{v} = 0, \quad (1)$$

$$\rho \frac{D\bar{v}}{Dt} = -\bar{\nabla} p + \mu \bar{\nabla}^2 \bar{v} + \bar{S}_M. \quad (2)$$

### 1.2.1 Flow Driven Motion with Six Degrees of Freedom (DOF) Solver

A rigid body is a solid object that moves through a fluid, while its shape remains undeformed. Its motion is dictated by the fluid forces and torques acting upon it and external forces (lift, gravity, friction) and external torques. In Ansys CFX [16] to [20] the computation of position and orientation of a rigid body is performed using equations of motion. The equations of motion of a rigid body are written as:

$$\vec{F} = \frac{d\vec{K}}{dt}, \quad \vec{M} = \frac{d\vec{L}}{dt} \quad (3)$$

These equations state that for a rigid body undergoing translation and rotation, the rate of change of its linear  $\vec{K}$  and angular momentum  $\vec{L}$  is equal to the applied force  $\vec{F}$  and torque  $\vec{M}$  acting on the body. The equation of motion for a translating center of a mass  $\bar{x}$  can be expressed using 2<sup>nd</sup> Newton law, where  $m$  is the mass and  $\vec{F}$  represents the sum of all forces. It includes hydrodynamic force, weight of rigid body, spring and explicit external force. Expanding the sum of all forces may be written as:

$$\sum \vec{F} = m \cdot \vec{a} = \vec{F}_{hydro} + m \cdot \vec{g} - k_{spring} \cdot (\bar{x} - \bar{x}_{SO}) + \vec{F}_{ext}, \quad (4)$$

where  $\vec{F}_{hydro}$  is hydrodynamic force,  $\vec{g}$  is gravity coefficient,  $k_{spring}$  is the linear spring constant,  $\bar{x}_{SO}$  is initial position coordinate and  $\vec{F}_{ext}$  are all other external forces acting on the body (buoyancy, friction). The flow force  $\vec{F}_{hydro}$  is the total component of the flow field acting on the body. It is determined from the RANS equations by integrating viscous wall shear stresses and pressure field over the body's surfaces:

$$\vec{F}_{hydro} = \sum (-p_i \cdot \vec{n}_i + \vec{\tau}_i) \cdot S_i. \quad (5)$$

The  $p_i$  denotes the pressure acting on the surface of a control volume whilst  $\vec{n}_i$  is the normal vector of the individual control volume face. The viscous stresses are denoted by  $\vec{\tau}_i$  and the surface of the control volume face is  $S_i$ .

The rigid body motion solution allows the turbine simulation with a flow driven approach, which means it can start to rotate from standstill due to water flow acting on its blades. Such an approach is convenient when we want to investigate whole turbine operation not just some constant conditions, where we would have to predict and define all the other operating parameters (e.g. angular velocity at a certain load).

### 1.2.2 Flow Driven Motion in Transient Sliding Grid Simulation with User Routine

The flow driven motion approach by using 6DOF solver shows relatively long computational times, but its major flaw is that it cannot be used in combination with FSI simulation. Therefore we developed our own user routine which enabled us to perform flow driven simulations using a less computational intensive but faster transient sliding grid method. Our routine was written using the Fortran programming language. There were two user routines needed, one that keeps

the angular velocity of a previous time step in external .txt file and another, which calculates the new angular velocity based on old one and difference in torque on turbine blades in the previous timestep. This result is then used as the rotating domain boundary condition. The equation for new angular velocity  $\omega_{new}$  is as follows:

$$\omega_{new} = \omega_{old} + \frac{(T - M_{load}) \cdot \Delta t}{J}, \quad (6)$$

where  $\omega_{old}$  is an angular velocity of a previous time step,  $T$  is the torque on turbine blades in a previous timestep,  $M_{load}$  is the loading moment,  $\Delta t$  is the timestep value and  $J$  is mass moment of inertia of a turbine rotor. This approach enabled us to perform flow driven simulation of Darrieus turbine using transient sliding grid procedure. The angular velocity of a turbine was updated in every time step, based on difference in torque on turbine rotor, loading moment and rotor moment of inertia. In such simulation, the turbine starts to turn due to the torque acting on a turbine rotor in every previous timestep as a consequence of a water flow.

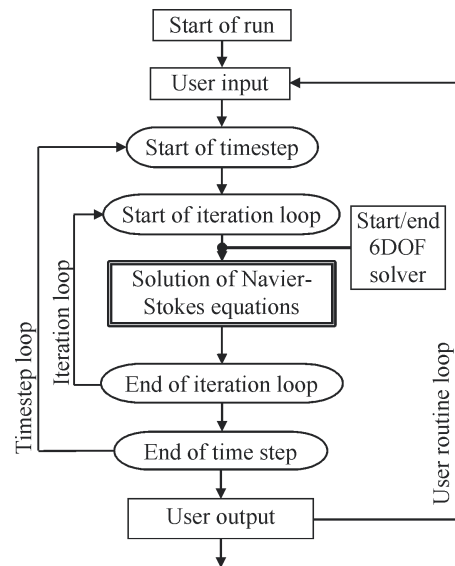


Fig. 2. Flow chart of a CFX simulation with rigid body solution and user CFX expression language (CEL) routine

From the simulation flowchart on Fig. 2, it can be observed that the user routine is called only once per timestep while CFX establishes a solution through iteration. Initially this was also the reason for instabilities in the early phase of simulation, because there is relatively large change of blade position in every timestep. This causes large pressure changes that produce high torque on the blades which is used

in further calculation of angular velocity, which moves the blades even faster. This means that there is self-amplifying effect, which drives the instability and can be reduced with certain measures. They are supposed to reduce large changes of results between timesteps, by applying smaller timesteps, starting a solution with a pre-simulated flow field around the blades, or decreasing change of angular velocity between time steps by applying a damp coefficient. For further use the simulation procedure has to be verified and validated with experimental results. For this purpose the results from experimental testing of water Darrieus turbine done by Shiono et al. [8] was used.

## 2 RESULTS AND DISCUSSION

### 2.1 Simulation Setup

Simulations with both flow driven approaches were performed on the same model in Ansys-CFX 13 [10]. The model of the Darrieus turbine with horizontal axis has three blades with the length of 0.2 and 0.3 m in diameter and corresponds to the experimental model used by Shiono et al. [8]. The rotating domain around the turbine is 0.45 m in diameter. It is modelled in a non-structured manner with 5,100,000 elements, which was determined by a preliminary mesh independence study, where results of present mesh differed from finer one by 2%. The upper and lower blade surfaces were modelled with 52 elements, with the smallest positioned around the leading and trailing edge, as can be seen on Fig. 3.

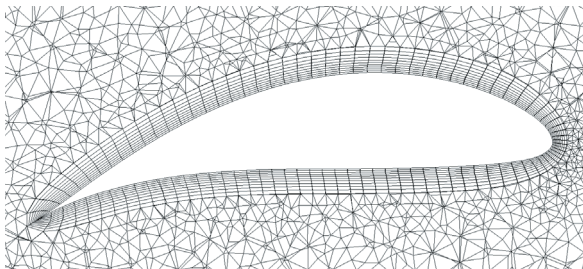


Fig. 3. Mesh distribution and boundary layer modeled around blade surface

The stationary domain around the turbine consists of 700,000 elements and extends one length of the diameter upstream, above and below the turbine and 2 diameters downstream in the wake field of a turbine, while its sides extend half of the blade length to the left and right side of the turbine. The aerodynamic profile of the blades is modified Naca 633018 profile

[5], with chord length of 126 mm which is projected on a circle with the diameter of 300 mm. The solidity,  $\sigma$ , states a relation between the blade area and the turbine swept area. For a Darrieus turbine it is defined as [8]:

$$\sigma = \frac{n \cdot C}{\pi \cdot D}, \quad (7)$$

where  $n$  represents the number of blades,  $C$  is the chord length of blade profile, and  $D$  is the turbine diameter. The solidity coefficient  $\sigma$  of model is 0.4 which corresponds to geometry tested by Shiono et al. [8].

The fluid model consisted of water at 10 °C and the turbulence model is two-equation  $k-\omega$  SST (shear stress transport) of Menter [17] and [18], with turbulence equations written in tensor form:

$$\frac{\partial(\rho k)}{\partial t} + \frac{\partial(\rho v_j k)}{\partial x_j} = P - \beta' \rho \omega k \frac{\partial}{\partial x_j} \left[ (\mu + \sigma_k \mu_t) \frac{\partial k}{\partial x_j} \right], \quad (8)$$

$$\begin{aligned} \frac{\partial(\rho \omega)}{\partial t} + \frac{\partial(\rho v_j \omega)}{\partial x_j} = & \frac{\gamma}{v_t} P - \beta \rho \omega^2 \frac{\partial}{\partial x_j} \left[ (\mu + \sigma_\omega \mu_t) \frac{\partial \omega}{\partial x_j} \right] + \\ & + 2(1 - F_1) \frac{\rho \sigma_{\omega 2}}{\omega} \frac{\partial k}{\partial x_j} \frac{\partial \omega}{\partial x_j}. \end{aligned} \quad (9)$$

Therefore, we used inflation modelling with 10 layers around each blade, which is required by that model [10].

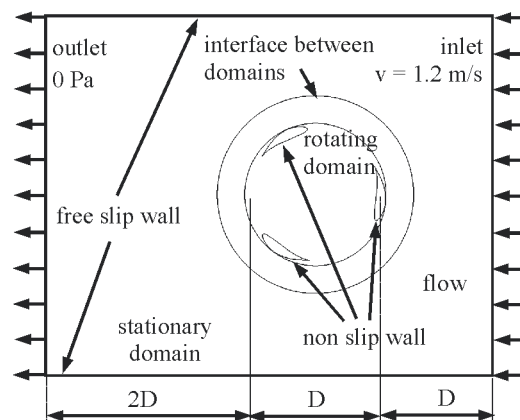


Fig. 4. Computational model of Darrieus water turbine and employed boundary conditions

The turbine surface is modelled as the 'non slip wall'. The top and the bottom surface of the test channel are prescribed as 'free slip wall' while the side surfaces has a 'symmetry' boundary condition. The water flow velocity is 1.2 m/s towards the turbine from the inlet on the front surface of stationary domain and the opposite surface, where the water exits, is modelled as 'outlet' with 0 Pa relative pressure (Fig. 4).

In order to acquire complete turbine power curve in a single simulation, simulation begins with water starting to flow and the turbine starts to rotate because of the water current acting on its blades. From the start of simulation there is a loading torque applied to a turbine rotor, which slowly increased from zero value with a rate specified by expression:  $T_{load} = 0.4 \text{ [Nm/s]} \cdot t$ , where  $t$  [s] is the simulation time. Several different rates were previously tested, so that turbine inertia does not affect the overall result. With such setup the turbine first reaches its maximum angular velocity, which slowly starts to decrease due to the constantly increasing load. As the simulation proceeds the load slowly becomes large enough to stop the turbine. With this simulation approach, it is possible to analyse the turbine efficiency over its whole operating range without the need to set several constant levels of loading. To compare several results of different analyses the results has to be transformed into dimensionless values. The angular velocity is usually represented as a tip speed ratio (TSR), which is a relationship between the turbine blade velocity and the current velocity [3]:

$$TSR = \frac{\omega \cdot R}{U_{\infty}} = \frac{v}{U_{\infty}}, \quad (10)$$

where  $\omega$  represents turbine angular velocity,  $R$  the turbine radius and  $U_{\infty}$  is the water current velocity. The available power of the water current  $P_{avail}$  can be calculated using following equation:

$$P_{avail} = \frac{1}{2} \cdot \rho \cdot A \cdot U_{\infty}^3, \quad (11)$$

where  $\rho$  is the water density and  $A$  is the free flow cross sectional area, which in our case corresponds to a turbine rotor swept area. The power of a hydrokinetic turbine  $P_{turb}$  is defined as:

$$P_{turb} = \omega \cdot T, \quad (12)$$

where  $T$  is the torque on a turbine shaft. The power coefficient  $C_p$  of a turbine which also represents its efficiency can be calculated as:

$$C_p = \frac{P_{turb}}{P_{avail}}. \quad (13)$$

The equation represents the relationship between power extracted from water current and power available in the current flowing through the same area as projected by the turbine. Hydrokinetic turbines extract energy from the fluid in a way that reduces the flow velocity with little or no pressure reduction as the fluid passes through the turbine rotor. Therefore, the current streamlines must expand to maintain continuity but they cannot expand indefinitely, so there is a theoretical limit to the amount of kinetic energy that can be extracted from the whole energy of a fluid. This limit has been determined by Betz [21] to be 59.3% for a surface through which energy is extracted.

## 2 RESULTS

We can observe the highly turbulent flow conditions [19] on the downstream side of a turbine, which are caused by its rotation. On Fig. 5 there are contours of fluid  $v_x$  velocities on inlet and outlet plane for two turbine positions (50 and 110°) with flow streamlines as well as corresponding flow fields in the middle section of the turbine rotor. On the downstream side there is strong downward vertical velocity, caused by blade traveling against the flow. The average value of turbulence kinetic energy  $k$  on the upstream side of the turbine is  $4.465 \cdot 10^{-3}$  J/kg and on the downstream side it is  $2.596 \cdot 10^{-2}$  J/kg. The dimensionless wall distance parameter  $y^+$  value during turbine operation was between 70 and 190, which is within the range recommended by best practice for turbomachinery simulation [16].

Both flow driven approaches has been used for turbine simulation. In both cases the turbine started to rotate due to water current from standstill, where in simulation with routine based flow-driven approach the torque on turbine blades and consecutive angular velocity oscillated strongly after it commenced, which can be seen on Fig. 6. Simulation became stable after two seconds and proceeded in a periodical pattern, similar to 6DOF-based simulation. The torque on the blades slowly increased and angular velocity decreased due to increasing load, where the angular velocity in routine-based simulation remains on a slightly higher level and has ~30% larger amplitude than in 6DOF-based simulation.

On Fig. 7, the torque on the turbine is shown for a single turn of a turbine during stable regular

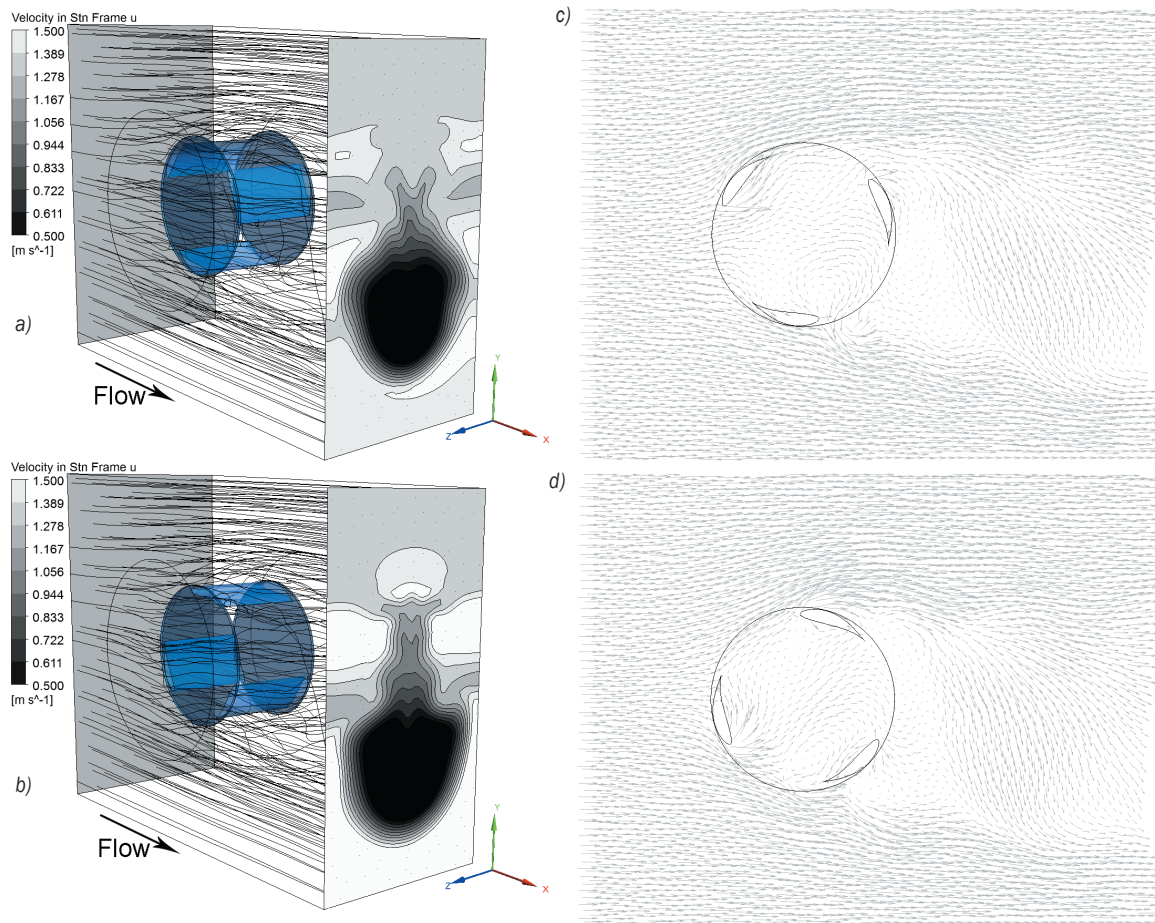


**Fig. 5.** The contours of flow  $v_x$  velocities on inlet and outlet of model and streamlines for two turbine positions, a) 50° and b) 110° and corresponding velocity vectors on a middle plane c) and d)

operation. The turbine has the same blade in its upmost position at the beginning and at the end of an interval. Therefore, the turbine positions in which its blades produce the most torque can be identified. It can be seen that the upmost blade starts producing torque from  $\sim 50^\circ$  onwards until it reaches  $\sim 100^\circ$  and that pattern is then repeated periodically for every  $120^\circ$  for a three bladed turbine.

The comparison of performance curves on Fig. 8 shows that routine-based flow-driven simulation over-predicts the experimental results by 11.3% while 6DOF-based simulation gives 3.1% higher result at peak tip speed ratio. The routine-based results however were following the trend of experimental results at nearly the same distance over the large part of the curve, while the 6DOF-based results were close to the experiment only at the peak value. The difference becomes larger in other areas. The main reason for difference in results between simulations and experiment is in the method by which Shiono

et al. [8] performed measurements. Their turbine was gradually loaded by electromagnetic brake and in each constant load level the rotating velocity and torque were measured, where the result represented an average value of a 30-second interval. In our simulations the turbine is loaded with constantly increasing torque, meaning that the turbine does not stabilize in a steady regular manner. Also the correct data of the test turbine, such as material and its mass moment of inertia as well as surface roughness were not available. Computationally, the difference between each simulation approach occurred because of differing flow-driven approaches. The 6DOF solver is involved in internal CFX iteration loop, so the solution of angular velocity is determined iteratively upon equilibrium, while in the approach with user routine, the angular velocity is updated only once per timestep. Therefore it represents certain disturbance, which is dependent on the rate of change of torque on the blades in a timestep. This is at its greatest at

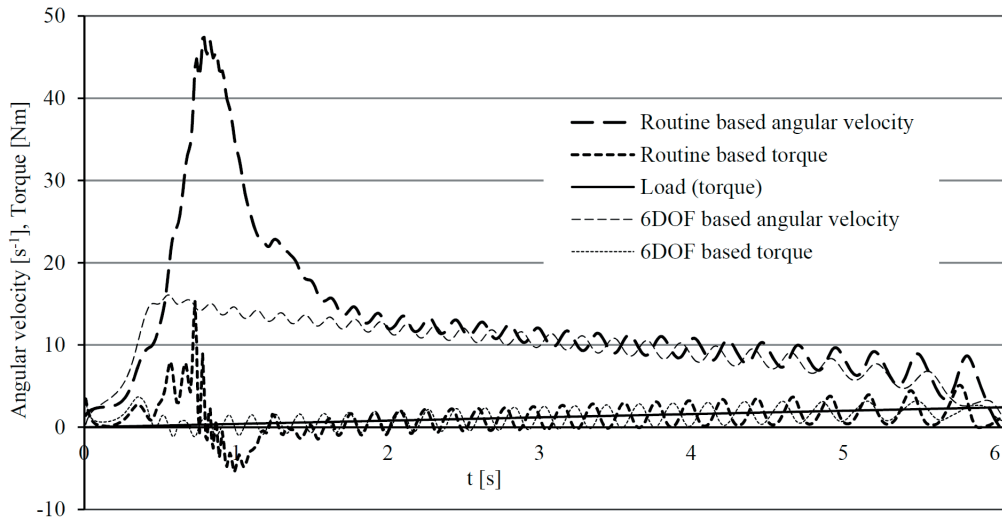


Fig. 6. Comparison of simulation results for 6DOF and user routine flow driven simulation approach

the beginning of the simulation, when the turbine accelerates from standstill to its highest angular velocity, therefore in first two seconds of simulation the large instability appears.

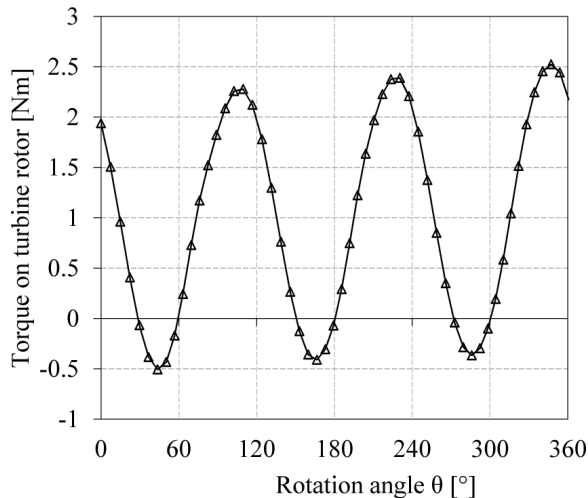


Fig. 7. Torque on a turbine rotor during its single turn, starting with one blade at  $\theta = 0^\circ$

The inertia in fluid field gathered in this period has certain influence on torque and angular velocity in the early phase of simulation. Also the turbine geometry used in the experiment has some influence on overall results of numerical simulation, due to its cross section with aspect ratio of 0.66. This means that the turbine blade length is one-third smaller than turbine diameter, so consequently the effect of turbine blades is reduced and the effect of supporting structure is increased.

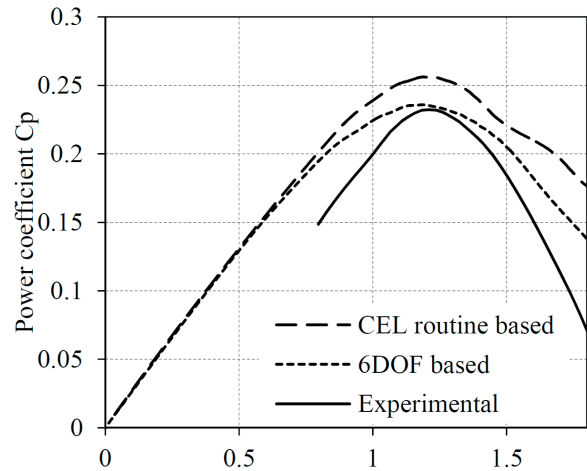


Fig. 8. Validation of computational model for both flow-driven approaches, compared to published experimental results

### 3 CONCLUSIONS

A new approach for fluid driven turbomachinery simulation was developed, enabling the analysis of a whole turbine operation range in a single simulation. The turbine simulations were performed with two approaches for flow-driven operation, where the turbine rotates due to the water stream acting on its blades. To capture its whole operation range, the turbine at the beginning of a simulation starts to rotate freely, after that, a gradually increasing load is applied, which slows the turbine rotation until it stops. Simulation results gathered with this procedure were well aligned to experimental results from the literature. The developed flow driven simulation approach is based on transient sliding mesh procedure

with an adaptive user routine, therefore it can be used in combination with strongly coupled FSI simulations. In this way in our further research the water current and the turbine could mutually interact, making it possible to analyse the influence of blade deformation on a turbine performance. For successful method application we would have to solve some issues regarding large instabilities at the start, which could cause some problems in FSI simulation due to large deformations under very high rotation velocities.

#### 4 ACKNOWLEDGEMENTS

This research was funded by SPIRIT Slovenia - Public Agency of the Republic of Slovenia for the Promotion of Entrepreneurship, Innovation, Development, Investment and Tourism.

#### 5 REFERENCES

- [1] Lago, L.I., Ponta, F.L., Chen, L. (2010). Advances and trends in hydrokinetic turbine systems. *Energy for Sustainable Development*, vol. 14, no. 4, p. 287-296, DOI:10.1016/j.esd.2010.09.004.
- [2] Yavuz, T., Kilkis, B., Akpinar, H., Erol, O. (2011). Performance analysis of a hydrofoil with and without leading edge slat. *Proceedings of the 10<sup>th</sup> International Conference on Machine Learning and Applications and Workshops, (Volume 2)*, p. 281-285, DOI:10.1109/ICMLA.2011.113.
- [3] Paraschivoiu, I. (2002). *Wind Turbine Design with Emphasis on Darrieus concept*. Polytechnic International Press, Montreal.
- [4] Darrieus, G.J.M. (1926). *Turbine Having Its Rotating Shaft Transverse to the Flow of the Current*. Patent 1835018. U.S. Patent and Trademark Office, Washington D.C.
- [5] Krauss, T. (2012). Airfoil Investigation Database, from <http://www.worldofkrauss.com>, accessed on 2012-09-20.
- [6] Islam, M., Ting, D.S.K., Fartaj, A. (2008). Aerodynamic models for Darrieus-type straight-bladed vertical axis wind turbines. *Renewable and Sustainable Energy Reviews*, vol. 12, no. 4, p. 1087-1109, DOI:10.1016/j.rser.2006.10.023.
- [7] Brahimi, M.T., Allet, A., Paraschivoiu, I. (1995). Aerodynamic analysis models for vertical-axis wind turbines. *International Journal of Rotating Machinery*, vol. 2, no. 1, p. 15-21, DOI:10.1155/S1023621X95000169.
- [8] Shiono, M., Suzuki, K., Kiho, S. (2000). An experimental study of the characteristics of a Darrieus turbine for tidal power generation. *Electrical Engineering in Japan*, vol. 132, no. 3, p. 38-47, DOI:10.1002/1520-6416(200008)132:3<38::AID-EEJ6>3.0.CO;2-E.
- [9] Fleisinger, M., Zadavec, M., Vesenjaj, M., Hriberšek, M., Udovičič, K. (2012). Comparison of CFD simulation of Darrieus water turbine using the rigid body solver and the MFR method. *Kuhljevi dnevi*, Slovensko društvo za mehaniko, Ljubljana. (in Slovene)
- [10] Malipeddi, A.R., Chatterjee, D. (2012). Influence of duct geometry on the performance of Darrieus hydroturbine. *Renewable Energy*, vol. 43, p. 292-300, DOI:10.1016/j.renene.2011.12.008.
- [11] McTavish, S., Feszty, D., Sankar, T. (2012). Steady and rotating computational fluid dynamics simulations of a novel vertical axis wind turbine for small-scale power generation. *Renewable Energy*, vol. 41, p. 171-179, DOI:10.1016/j.renene.2011.10.018.
- [12] Yang, B., Lawn, C. (2011). Fluid dynamic performance of a vertical axis turbine for tidal currents. *Renewable Energy*, vol. 36, no. 12, p. 3355-3366, DOI:10.1016/j.renene.2011.05.014.
- [13] Rossetti, A., Pavesi, G. (2013). Comparison of different numerical approaches to the study of the H-Darrieus turbines start-up. *Renewable Energy*, vol. 50, p. 7-19, DOI:10.1016/j.renene.2012.06.025.
- [14] Intel Corporation (2010). Intel® Fortran Compiler 11.1 User and Reference Guides, from [http://nf.nci.org.au/facilities/software/FORTRAN/Intel11.1/en\\_US/compiler\\_f/main\\_for/index.htm](http://nf.nci.org.au/facilities/software/FORTRAN/Intel11.1/en_US/compiler_f/main_for/index.htm), accessed on 2014-02-03.
- [15] Howell, R., Qin, N., Edwards, J., Durrani, N. (2010). Wind tunnel and numerical study of a small vertical axis wind turbine. *Renewable Energy*, vol. 35, no.2, p. 412-422, DOI:10.1016/j.renene.2009.07.025.
- [16] Ansys (2010). *Ansys CFX - Solver Theory Guide*. Ansys, Inc., Canonsburg.
- [17] Hriberšek, M., Škerget, L., Poredoš, A. (2005). *Process Engineering. Part 1, Basics, Mixing, Drying*. University of Maribor, Faculty of Mechanical Engineering, Maribor. (in Slovene)
- [18] Menter, F., Langtry, R., Völker, S., Huang, P. (2005). Transition Modelling for General Purpose CFD Codes. *Engineering Turbulence Modelling and Experiments 6: Proceedings of the International Symposium on Engineering Turbulence Modelling and Measurements*, Sardinia, p. 31-48, DOI:10.1016/B978-008044544-1/50003-0.
- [19] Kraemer, K. (1961). *Flügelprofile im kritischen Reynoldszahl - Bereich*. Aerodynamische Versuchsanstalt, vol. 27, no. 2, p. 33-46.
- [20] Simo, J.C., Wong, K.K. (1991). Unconditionally stable algorithms for rigid body dynamics that exactly preserve energy and momentum. *International Journal for Numerical Methods in Engineering*, vol. 31, no. 1, p. 19-52., DOI:10.1002/nme.1620310103.
- [21] Betz, A. (1920). Das Maximum der theoretisch möglichen Ausnützung des Windes durch Windmotoren. *Zeitschrift für das gesamte Turbinenwesen*, vol. 26.